Chapter 10

Photogeologic Maps of the 2004–2005 Mount St. Helens Eruption

By Trystan M. Herriott[1], David R. Sherrod[2], John S. Pallister[2], and James W. Vallance[2]

Abstract

The 2004–5 eruption of Mount St. Helens, still ongoing as of this writing (September 2006), has comprised chiefly lava dome extrusion that produced a series of solid, fault-gouge-mantled dacite spines. Vertical aerial photographs taken every 2 to 4 weeks, visual observations, and oblique photographs taken from aircraft and nearby observation points provide the basis for two types of photogeologic maps of the dome—photo-based maps and rectified maps. Eight map pairs, covering the period from October 1, 2004, through December 15, 2005, document the development of seven spines: an initial small, fin-shaped vertical spine; a north-south elongate wall of dacite; two large and elongate recumbent spines ("whalebacks"); a tall and elongate inclined spine; a smaller bulbous spine; and an initially endogenous spine extruded between remnants of preceding spines. All spines rose from the same general vent area near the southern margin of the 1980s lava dome. Maps also depict translation and rotation of active and abandoned spines, progressive deformation affecting Crater Glacier, and distribution of ash on the crater floor from phreatic and phreatomagmatic explosions. The maps help track key geologic and geographic features in the rapidly changing crater and help date dome, gouge, and ash samples that are no longer readily correlated to their original context because of deformation in a dynamic environment where spines extrude, deform, slough, and are overrun by newly erupted material.

Introduction

During its 2004–5 eruptive activity, Mount St. Helens extruded solid dacite lava onto the May 18, 1980, glacier-covered crater floor south of the 1980s lava dome. Beginning in October 2004, a series of seven spines extruded during the first 15 months of the eruption, following seismic unrest that began September 23, 2004. Two prominent whaleback-shaped spines (3 and 4) that erupted from late October 2004 to April 2005 followed two small spines (1 and 2) extruded in October 2004. From April through July 2005, tall, inclined spine 5 overrode remnants of previous spines to reach the dome's maximum altitude as of September 2006 (Schilling and others, this volume, chap. 8); this spine subsequently subsided and partially disintegrated. Finally, beginning in early August 2005, spines 6 and 7 extruded westward, a marked change from previous spines, which were shoved south along the crater floor. Remnant spines (those no longer actively extruding) were rapidly degraded and over-run by subsequent spines. Crater Glacier, which formed after the cataclysmic 1980 eruption (Schilling and others, 2004; Walder and others, this volume, chap. 13), was nearly bisected during the initial two months of the eruption and formed distinct east and west limbs that were substantially deformed in response to emplacement of the new lava dome.

Intensive monitoring of the eruption by the U.S. Geological Survey's Cascades Volcano Observatory (CVO) has been supplemented by photographic documentation of the dome's growth (this volume: Poland and others, chap. 11; Major and others, chap. 12; Dzurisin and others, chap. 14), including a series of 9×9-in. vertical aerial photographs. We present eight photogeologic maps traced from vertical aerial photographs of the Mount St. Helens crater that encompass 15 months of the eruption from October 1, 2004, through December 15, 2005. Each map is presented as both a photo-based and an accompanying rectified map without a photo base. The maps depict (1) the growth, stagnation, and subse-quent burial or degradation of seven dacite spines (fig. 1); (2) the translation and rotation of geologic and geographic features throughout the evolution of the ongoing dome eruption; and (3) the progressive deformation of Crater Glacier as the growing dome displaced ice south of the 1980–86 dome. The photo-based maps also serve as a base for plotting locali-

[1] Department of Earth Science, Webb Hall, University of California, Santa Barbara, CA 93106; now at P.O. Box 750255, Fairbanks, AK 99775

[2] U.S. Geological Survey, 1300 SE Cardinal Court, Vancouver, WA 98683

ties of, and giving geologic and geographic context to, rock, gouge, and ash samples that were collected on the growing lava dome. Photographic documentation of sample context is crucial in a constantly changing setting in which a sample's original location loses significance, as when the base of a coherent spine sampled in January 2005 becomes a pile of transported and undifferentiated rubble by May 2005.

Methods

We compiled maps of the 2004–5 dacite dome eruption at Mount St. Helens on a sequence of ~1:12,000-scale vertical aerial photographs taken by Bergman Photographic Services on contract to CVO (Schilling and others, this volume, chap. 8). Photo pairs encompassing the crater rim, new lava dome, and the 1980–86 lava dome were selected and examined with a stereoscope. The crater rim and 1980s lava dome provided a reasonably stable frame of reference in the dynamic crater environment. On the photographs we mapped units that highlighted changes in dome growth and morphology, as well as changes in the 1980s dome, rock debris, and glacial ice surrounding the dome. Uncertainties of the map units result from working without the benefit of on-the-ground field mapping, which early in the eruption was deemed too hazardous owing to possible explosions or rockfalls and rock avalanches. Our intent is to provide a heightened visual record of the locations and characteristics of major features and deposits in the crater during the ongoing eruption.

Two types of photogeologic maps were prepared—photo-based and rectified. The latter lacks a base image in its final presentation. The visual content of the aerial photographs is immense, and unit boundaries are commonly vivid; however, the aerial photographs are not rectified, and therefore the photo-based maps are subject to scale variability and distortion within an individual image. Consequently, areas of, and distances between, map units on the photo-based maps are only comparable qualitatively. The rectified geologic maps allow quantitative comparison and complement the visually rich, nonrectified photo-based maps.

Although the two map series are based on the same photo pairs for any given date, variations exist within each map pair (photo-based and rectified). Dissimilarities result primarily from compiling the two types of maps at separate times but are compounded by employing different methods for assessing the contact locations (see below). Without doubt, the greater magnification and clarity possible with the plotter used to make the rectified maps resulted in a finer degree of detail, especially in differentiating gouge-covered surface, unroofed spine, and talus. Ultimately, small differences within map couplets persist. The two map series are not intended to be rigorously comparable but rather to be viewed and used for their individual strengths as discussed above.

Photo-Based Geologic Maps

We selected photographs on the basis of observable changes since previous photo coverage, visual clarity of crater
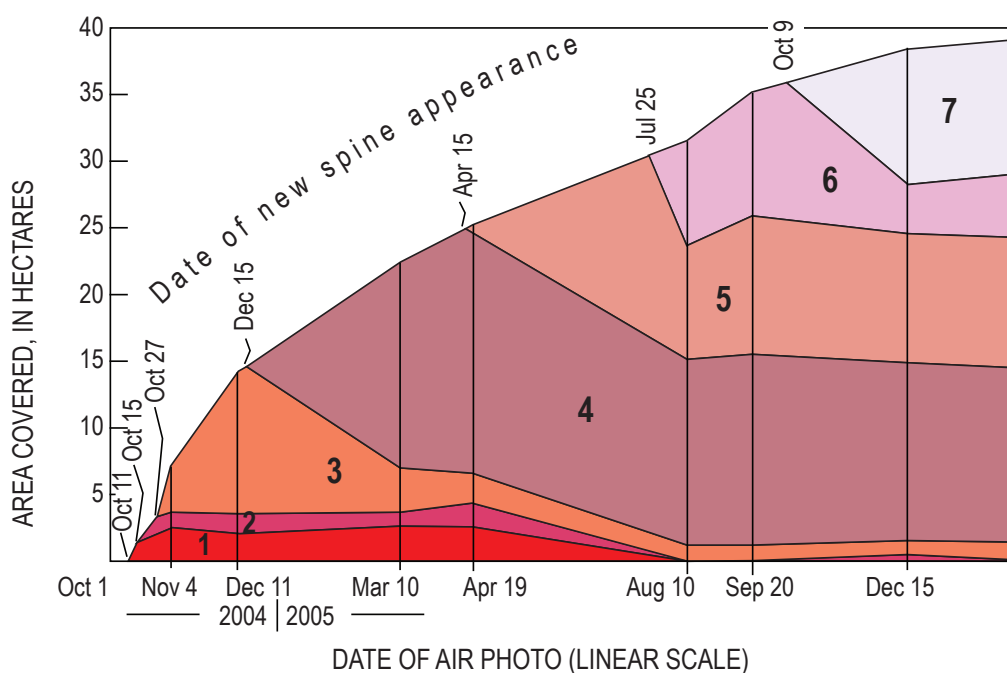

Figure 1.   Area of Mount St. Helens' new dome and proportional coverage of individual spines through time. Areas measured from rectified photogeologic maps produced for dates of air photos shown. Date of new spine appearance from Vallance and others (this volume, chap. 9).

Table 1. Imagery used for photogeologic maps.

[Photo number (ex: 6-5) reported as flightline and frame number. Samples are whole-rock and gouge samples used for geochemical analyses described elsewhere in this volume. For brevity, sample numbers lack "SH" prefix (for example, complete sample No. is SH300). For stereographic pair, first listed is left-hand photo, southerly of pair; all flightlines oriented north-south. Column for georegistration points indicates number of points used in transformation to better rectify the photogrammetric geologic map.]

Date of pho-tography	Figure No.	Photo used	Samples shown on photo map	Pair used for rectified map	Georegis-tration points
10/1/2004	2, 3A	6-5	No new dome	6-4, 6-5	19
11/4/2004	4, 3B	6-4	300, 301-1, 302-2, 304-1, 304-2	6-3, 6-4	15
12/11/2004	5, 3C	6-3	305	6-2, 6-3	19
3/10/2005	6, 3D	7-2	306, 307, 308, 309, 310, 311-1B, 312	7-2, 7-1	10
4/19/2005	7, 8A	6-4	313, 314, 315, 316	6-3, 6-4	19
8/10/2005	9, 8B	1-3	317, 318, 319, 320, 321, 322, 323	1-2, 1-3	22
9/20/2005	10, 8C	1-2		1-2, 1-3	15
12/15/2005	11, 8D	1-3	324	1-2, 1-3	25

features, and pertinence to appropriate geographic setting of sample localities. These selection criteria winnowed the aerial photograph series from 18 to 8 sets (table 1). Our procedure began by scanning (300 dpi) each of the chosen set of photographs. The scanned images were enlarged and framed to encompass a similar area at roughly similar scale. We then traced rock, ash, and glacier units using Adobe ® Illustrator 10 software. Although the photo-based maps are neither rectified nor georeferenced, we attempted to maintain the same field of view and azimuthal orientation (top to the north) of maps throughout the photo-based series.

We studied photo pairs stereoscopically and analyzed apparent three-dimensional surface morphology to identify photogeologic features and draw detailed map-unit contacts. Dashed lines on the maps indicate ambiguous contact locations. Thermal imagery and digital elevation models (DEMs) constructed from each set of photos (Schilling and others, this volume, chap. 8; Vallance and others, this volume, chap. 9) augmented the interpretation of geologic features and deposits viewed on the aerial photographs. We resolved additional crater details by referring to the extensive collection of oblique aerial photographs taken in the crater during field work by CVO scientists and by comparing aerial photographs with repeat images from time-lapse cameras at three fixed locations near the crater rim (this volume: Poland and others, chap. 11; Major and others, chap. 12; Dzurisin and others, chap. 14). These supplementary data elucidate areas within the crater that are obscured in the aerial photographs by condensed steam, shadows, or snow, or are difficult to interpret in plan view.

Rectified Geologic Maps

Conventional photogrammetric methods were used to rectify photogeologic maps. We mapped contacts while viewing paired vertical aerial photos stereoscopically on a Kern PG-2 optical-mechanical stereographic plotter. Our instrument at CVO lacks an electronic digitizer, so the resulting pencil-on-mylar maps were scanned and hand digitized using MapInfo ® Geographic Information System (GIS) software. Points of known geographic position, such as prominences on the crater rim and on the 1980s dome within the crater, served as pseudobenchmarks by which the maps were registered geographically. The crater-rim control points are prominent apices and craggy summits whose locations were derived from a lidar image with 2-m cells produced in November 2004. The 1980s-dome control points are rock spires recognizable on a 1988 high-resolution topographic map of the crater floor.

The PG-2 plotter produced rectified maps under most conditions; however, the photos encompass substantial altitude variation, more than 600 m, across short horizontal distances. Parallax-free models are therefore difficult to achieve, and a small amount of distortion may occur in the resulting maps. The problem is exacerbated by using the crater rim for geographic registration, whereas the area of geologic interest lies entirely on the crater floor, substantially lower in altitude. Moreover, snow cornices modify the crater rim in winter, with some forming prominent topographic apices recognizable in DEMs and aerial photos; these windblown snow and ice features can rebuild in slightly different geographic positions from photo to photo, a source of error for which we cannot system-

atically account. The crater rim itself retreats episodically by erosion, but no noticeable changes caused by this effect were observed in the 15 months that span our geologic maps.

To minimize distortion, the scanned pencil-on-mylar images were transformed by rubbersheeting methods. Specifically, the image was brought into its approximately correct position by a transformation matrix (general perspective projection transformation) and then by triangular irregular net adjustment (for fuller discussion of methodology, see Schilling and others, this volume, chap. 8). The transformations involved 15 to 25 registration points, except for the imagery of March 10, 2005, which used 10 points (table 1).

Ultimately, the resulting precision and probably the accuracy of the rectified maps is within plus or minus 12 m. This value is acceptable owing to the 1:12,000 scale of the aerial photographs and the standard convention that a geologic map should portray precision to at least 1 mm on the map. The precision was tested empirically by draping the resulting linework on existing DEMs. The crater rim was traced as part of each rectified map to provide a visual-empirical guide for comparison with the crater rim on the DEM. Rock spires on the 1980–86 dome provided intracrater tie points to further assess precision. The crater-rim test shows that all tracings lie within 5 m of each other. As a test of accuracy, the rock-spire test gives geographic coincidence generally within 1–5 m, with a few strays as far as 10 m. The resulting rectified maps are more than adequate, in both precision and accuracy, for the cataloging and archiving of geologic information.

Sample Localities

CVO staff collected (chiefly by helicopter dredge) and analyzed 26 samples of 2004–5 lava-dome dacite after the first dacite spine erupted in mid-October 2004 (Pallister and others, this volume, chap 30; Thornber and others, 2008). Sample localities (table 1) are plotted on the photo-based maps that depict relevant geologic and geographic features, providing approximate spatial and temporal context for the samples.

Description of Photogeologic Map Units

Map units described here include rock and debris from the 2004–5 dacite dome, phreatic or phreatomagmatic and rockfall-generated ash deposits, crater floor debris, 1980s lava dome, and deformed and undeformed glacial ice. Labels coupled with a plus sign (+) indicate where thin surficial deposits blanket other map units. The underlying map unit is listed first, followed by the symbol of the blanketing deposit. For example, unit label gd+a indicates deformed glacier overlain by a veneer of ash (see Dome Map Units, below).

We use lava dome, or simply dome, to describe the composite feature that comprises extrusive spines or lobes,

endogenous growth, and talus. We mapped each spine as an individual unit of extrusive lava, typically massive, and analogous to a lobe or flow. Endogenous growth of some spines results in a rubbly surface. A whaleback is a smooth, striated spine, be it recumbent or vertical. The terms "new" and "old" dome are used informally to differentiate between the 2004–5 and 1980–86 lava domes, respectively.

The term Opus identifies an informally named part of the 1980s dome that was displaced southward during a 1985 eruption. The name originated from a benchmark used to track this movement and later was extended through casual usage to denote the entire elongate geographic ridge that resulted. Opus became important during the renewed eruption in 2004 because the conduit breached the surface near it, deforming both Opus and the adjacent Crater Glacier.

Crater Glacier deformed because of upwarping early in the eruption and then by lateral compression as extruded lava shoved the glacier aside. We demarcate deformed and undeformed glacial ice by tracing the abrupt topographic break in slope between them. This boundary was a deformation front within a compositionally coherent unit, unlike lithologic contacts, which are planar features separating discrete bodies of rocks or deposits.

2004–2005 Dacite Dome Map Units

Spines—Lava lobes, numbered 1–7 according to eruptive sequence of dacite lava extruded onto floor of Mount St. Helens crater during eruption ongoing since October 2004 (Vallance and others, this volume, chap. 9). Moderately porphyritic, with phenocrysts of plagioclase, amphibole, hypersthene, and Fe-Ti oxides. Includes three gross textural features— surface gouge; unroofed, ragged spine; and remnant spine—described below. Thus, map symbol may be a composite; for example, s4u indicates unroofed, ragged part of spine 4 after erosion has destroyed its smooth carapace. Spines defined as follows:

s7 Spine 7—Initially endogenous dacite spine; extruded between remnants of spines 5 and 6 beginning in October 2005. Longest-lived and latest in sequence as of September 2006

s6 Spine 6—Rubble-covered dacite spine; extruded during August and September 2005. Grew coincident with and adjacent to a graben, or sag, that developed west of spine 5

s5 Spine 5—Large south-trending dacite spine; extruded from late April through July 2005. Highest spine measured as of September 2006 (Schilling and others, this volume, chap. 8)

s4   Spine 4—Large, elongate, south-trending dacite whaleback; extruded from late December 2004 through late April 2005

s3   Spine 3—Large, elongate, south-trending dacite whaleback; extruded from late October through late December 2004. First occurrence of gouge-mantled spine with striated carapace, characteristic of all subsequent spines

s2   Spine 2—Elongate south-trending dacite spine; extruded in middle to late October 2004

s1   Spine 1—Small northeast-trending finlike dacite spine; initial effusive product; extruded in mid-October 2004

u   Unroofed spine—Part of actively growing spine that no longer retains gouge-mantled carapace, which typically was shed through repeated rockfalls

r   Spine remnants—Partially intact rubble of inactive spines. Moved constantly as growth of new spine wedged them away from vent

g   Gouge—Cataclastic carapace 1–2 m thick that characterized surfaces of spines 3–7 where they first emerged from the vent. Commonly removed by fracturing and degradation

t   Talus—2004–5 dacite dome talus resulting from rockfall from active and abandoned spines. May be darker in color than adjacent hot talus where wet or covered by damp ash

a   Ash—Tephra, produced chiefly by phreatic or phreatomagmatic explosions and rockfalls. Shown separately on some maps are the following units:

a2   Ash from March 8, 2005, explosion—Primary magmatic and accidental lithic tephra generated during largest phreatomagmatic explosion of ongoing eruption. Resulted from near-vent fallout from plume of steam and ash that rose to about 11 km height

a1   Ash from October 1, 2004, explosion—Fine ash that blanketed northwest sector of Mount St. Helens crater

v   Vent for October 1, 2004, explosion—Pit about 50 m in diameter that produced a short-lived steam-and-ash plume of phreatic or phreatomagmatic origin. Source of first explosive activity of ongoing eruption

b   Ballistic craters—Depressions in glacier caused by bomb impacts during October 1, 2004, and March 8, 2005, explosions

Other Crater Map Units

rp   Crater-floor roof pendant—Crater-floor debris that rested atop spine 3 upon its initial extrusion

gl   Crater Glacier—Glacial ice and enclosed rock debris that accumulated subsequent to May 18, 1980, crater-forming eruption. Compression and thickening by crater-floor uplift and extrusion of new lava dome increased rate of flow northward around 1980s dome. Shown separately are the following:

gd   Deformed Crater Glacier—Deformed, typically uplifted and crevassed glacial ice shoved aside as lava dome grew

gs   Stranded glacial ice—Remnant of ice from east glacier left perched on flank of Opus by crater-floor uplift

la   Lahar deposits—Remnants of small muddy debris flows and tiny pyroclastic flows generated by interaction of hot dacite dome rock and snow or glacial ice

cd   Crater-floor debris and talus—Rubble uplifted by actively growing 2004–5 dacite dome

cw   Crater wall—Strata forming crater walls and outer flanks of Mount St. Helens. Unit only appears on rectified maps

op   Opus—Ridge created on south side of 1980s dome by a small graben that formed during October 1985 eruption

od   1980–86 lava dome—Older dome emplaced during a 6-year period following the May 18, 1980, crater-forming eruption

h   Melt pit—Steeply walled pits at glacier/lava dome contact melted out by fumaroles. Unit only appears on rectified maps

*   2004–5 sample location—Sample location, showing number (for example, 300; the SH prefix is not included in the map label); most samples collected by helicopter dredging tools. Shown only on photo-based maps

Discussion of Photogeologic Maps

Our discussion of the maps focuses on salient geologic, geographic, topographic, and glacial features generated during the first 15 months of the eruption. These include spine evolution, phreatic and phreatomagmatic explosions, uplifted crater-floor rocks, deformation of Opus, deformation of the Crater Glacier, and extensive rockfall-generated ash deposits. We do not discuss all features depicted in the images, as our goal is to provide a guide for visualizing the most notable changes on the crater floor between the dates of successive maps.

October 1, 2004

The October 1 phreatic explosion left its mark on the crater scene photographed that afternoon (fig. 2). Dark-gray ash (a1) mantles the western crater floor, having emanated from a prominent vent (v) in the Crater Glacier. Numerous craters on west Crater Glacier define a more restricted field of ballistic craters (a1b).

Adjacent to the vent on the east is highly fractured and uplifted glacial ice (gd), a welt approximately 52,000 m^2 in extent that grew rapidly as magma ascended toward the surface (fig. 3A). The base of the topographic rise to the welt, distinctive in stereo viewing but not readily apparent in the single base image of figure 2, defines the contact separating deformed from undeformed glacier. With time, some of the deformed ice seen in figure 2 became isolated from the main mass of Crater Glacier. The Opus ridge (op) is also deformed.

November 4, 2004

The November 4 image shows spine 3 (s3) and remnants of spines 1 (s1r) and spine 2 (s2r) of the new dome (fig. 4). The east-flank carapace of spine 3 is a well-preserved striated gouge surface (s3g). A distinctly whiter band marks the freshest gouge along the eastern base. Remnants of spines 1 and 2 are north and west, respectively, of spine 3.

At least one roof pendant (rp) of old dome and crater-floor debris is atop spine 3. In the photo, the pendant is seen as the darker area near the crest of the spine (fig. 4). Dark-gray

Figure 2.   Photo-based geologic map of Mount St. Helens' new dome from aerial photo taken October 1, 2004. For explanation of unit symbols, see text. Shoestring notch is an informal geographic name for the topographic cleft that is the truncated head of the Shoestring Glacier, which was largely destroyed in the 1980 eruption of Mount St. Helens.

debris (cd) along the eastern periphery of spine 3 represents deformed fragments of the 1980–86 dome, first dragged southward 100–200 m on the roof of spine 3 and then eroded off (fig. 3*B*). Uplifted crater floor material lies east of the 1980s dome debris (fig. 3*B*).

East of the new dome is the highly deformed east limb of Crater Glacier (gd), crisscrossed by crevasses to form a serac field. The growing dome has nearly split the glacier, such that its east and west limbs have become geographically distinct. Nevertheless, the glacier remains contiguous around the south side of the new dome.

Deformation of Opus (op) is largely complete but is not easily discerned at the scale of this aerial image (fig. 4); stagnant and broken glacial ice mantles its south side. Increased heat flow on its western side has melted snow from an irregular area, but the exposed, darkened mass of jumbled rock is likely little different in form from the snow-covered nonthermal area of Opus.

Two or three small debris fans and more lobate, slurried deposits (la) originate from spine 1 remnants. Thinner lahar deposits extend along a narrow trace down the center of the cleft that separates the west flanks of the new and 1980s domes from the west limb of Crater Glacier (gl) (fig. 4).

December 11, 2004

Rain, melted snow, or condensed steam has left the snow-free areas very dark gray on this overcast day (fig. 5). Spine 3 has greatly lengthened, earning the name "whaleback." Its gouge-mantled surface (s3g), where wet, is dark grayish brown. The western slope of spine 3 has spalled to form talus (t), including some large house-size blocks. All the uplifted crater-floor debris seen along the west flank in previous images is now indistinguishable, likely buried by talus. Along the southeast side, steam and coarse blocks mark an elongate slab of spine 3 (s3u), detached, deformed, and wedged between spine 3 and the glacier (fig. 3*C*). Spine 1 and 2 remnants remain visible, although they are somewhat obscured by steam in this image (fig. 5).

Notable deformation continues on the east limb of Crater Glacier (gd), but only small changes occur along its west limb. The glacier remains intact along the south side of the new dome, but it has narrowed greatly to only about 60 m (fig. 3*C*). Glacial ice on parts of Opus has disappeared, causing an expansion of the area of Opus (compare figs. 3*B*, 3*C*).

March 10, 2005

Geomorphically prominent spine 4 has by this time supplanted spine 3, which underwent rapid fragmentation during early January 2005 (fig. 6). Spine 4 evolved as the northernmost part of spine 3 split along a vertical fracture and decoupled at its root from the rest of spine 3 to the south. As it grew southward, spine 4 isolated a small relic of spine 3 (s3ru) to the west as it bulldozed the remainder to the east (Vallance and others, this volume, chap. 9); these remnants emit steam where they abut glacial ice along the east margin.

The stunning striated and gouge-mantled carapace of spine 4 (s4g), as well as the crevassed and thickened tongue of the deformed glacier (gd, east of spine 4; see below), take center stage in this photo. Remnants of spines 1 and 2 are increasingly ragged in appearance. Virtually no uplifted crater-floor debris remains adjacent to the new spines, as it has been buried by talus (t).

A large phreatomagmatic explosion on March 8 distributed ash (a2) across the north and east sectors of the crater, but large ballistic fragments fell chiefly north and northwest of the new dome. Opus and its shroud of snow and ice lie pinched between the new and 1980s domes. The stagnant ice on Opus (unit gs on fig. 3*D*) is now fully separated from the actively deforming glacier.

The east limb of Crater Glacier deformed dramatically through March and into April, producing the prominent, lobate deformation front visible near the southeast margin of the 1980–86 dome. The amplified glacial deformation slowed significantly in subsequent weeks.

April 19, 2005

Spine 5 (s5) at this time lies at the north end of the spine 4 whaleback remnants, with much of its gouge-covered surface (s4rg still intact (fig. 7). Extensive sloughing of spine 4 was first observed following a 2-week stormy period in late March 2005. Spine 4's southward growth and collision with the southern crater wall caused its breakup. Spine 3 (s3ru) is reduced to remnants flanking spine 4. Spine 1 and 2 remnants persist, although spine 2 (s2r) steams vigorously where shoved into the western limb of the glacier, so that little of it is visible in this photo (fig. 7).

Snowfall subsequent to the March 8 phreatomagmatic explosion buried the thin veneer of ash and ballistic fragments from that event. Distinctive ash (a) blanketing the east limb of the crater glacier on this image is a localized deposit that resulted from a large hot rockfall off the northeast face of spine 4 remnants (fig. 8*A*). Blocky rockfall material stopped abruptly at a topographic rise on the deformed east glacier; the rise is well pronounced in stereo viewing, but not readily apparent in figure 7. Ash elutriated and surged ahead for a short distance, forming the darkest of the deposit seen in the photo (gd+a, northern extent) (fig. 7). Even finer ash traveled south, presumably downwind, before being deposited (gd+a, southern extent).

August 10, 2005

Spine 6 (s6) separates from spine 5 at this time and edges westward (fig. 9), contrasting with previous spines that pushed along a south-southeastward trajectory. This new growth pattern focuses deformation of Crater Glacier in its west arm. The heretofore relentlessly moving terrain of spine 3, 4, and 5 remnants stagnates over the next few months (compare spatial relations in figs. 8*B*, 8*C*, 8*D*). Spine 3 remnants (s3ru) are vis-
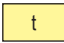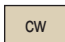
Figure 3.   Rectified geologic maps of Mount St. Helens' new dome. *A,* October 1, 2004. *B,* November 4, 2004. *C,* December 11, 2004. *D,* March 10, 2005.

EXPLANATION

FEATURES ASSOCIATED WITH NEW DOME

s3u / s3g	Spine of 2004–2005 eruption (ongoing in December 2005)—Darker area mantled by gouge
t	Talus from flank of spine
la	Lahar deposits from area of new dome
cd	Crater-floor debris
	Wedge of downdropped crater-floor debris
	Vent for phreatomagmatic eruption of October 1, 2004

TEPHRA DEPOSITS ON MAP OF MARCH 10, 2005

──── Distribution of coarse ballistics—Dashed where lack of snow cover makes limit of cratering indistinct

- - - Northern and southern limits of lapilli and ash

TEPHRA DEPOSITS ON MAP OF OCTOBER 1, 2004

──── Ash distribution

Ballistic fallout
──── Inner, dense fall
- - Outer limit of sparse fall

OTHER FEATURES IN CRATER

h	Melt pit at glacier margin
	Talus from crater walls and 1980–86 dome
gl / gd	Glacial ice—Darker area deformed by dome growth
od / op	1980–86 dome—Darker area is Opus ridge (op)
cw	Strata of crater walls and outer flanks
────	Notable crevasse on glacier—Resulting from dome emplacement. Only crevasses that developed after the previous map date are shown

Figure 3.—Continued.

Figure 4.   Photo-based geologic map of Mount St. Helens' new dome from aerial photo taken November 4, 2004. Stars mark sample localities; see table 1.
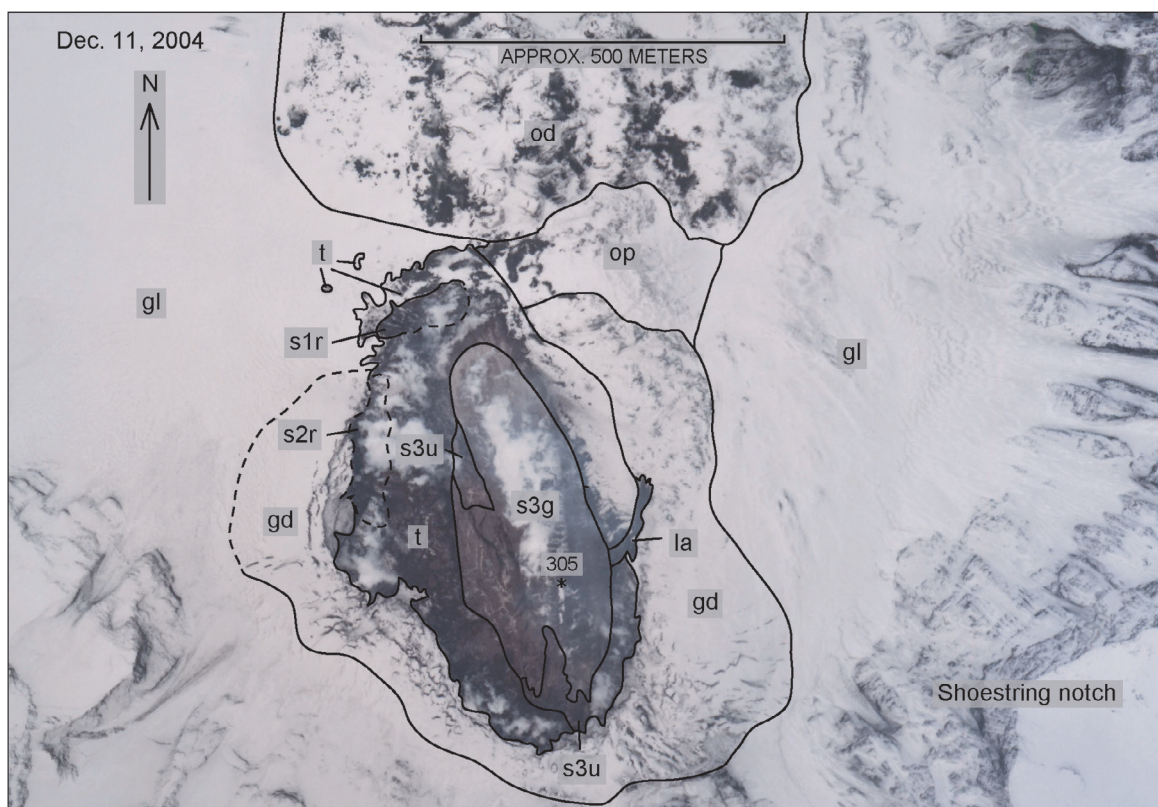

Figure 5.   Photo-based geologic map of Mount St. Helens' new dome from aerial photo taken December 11, 2004. Star marks sample locality; see table 1.
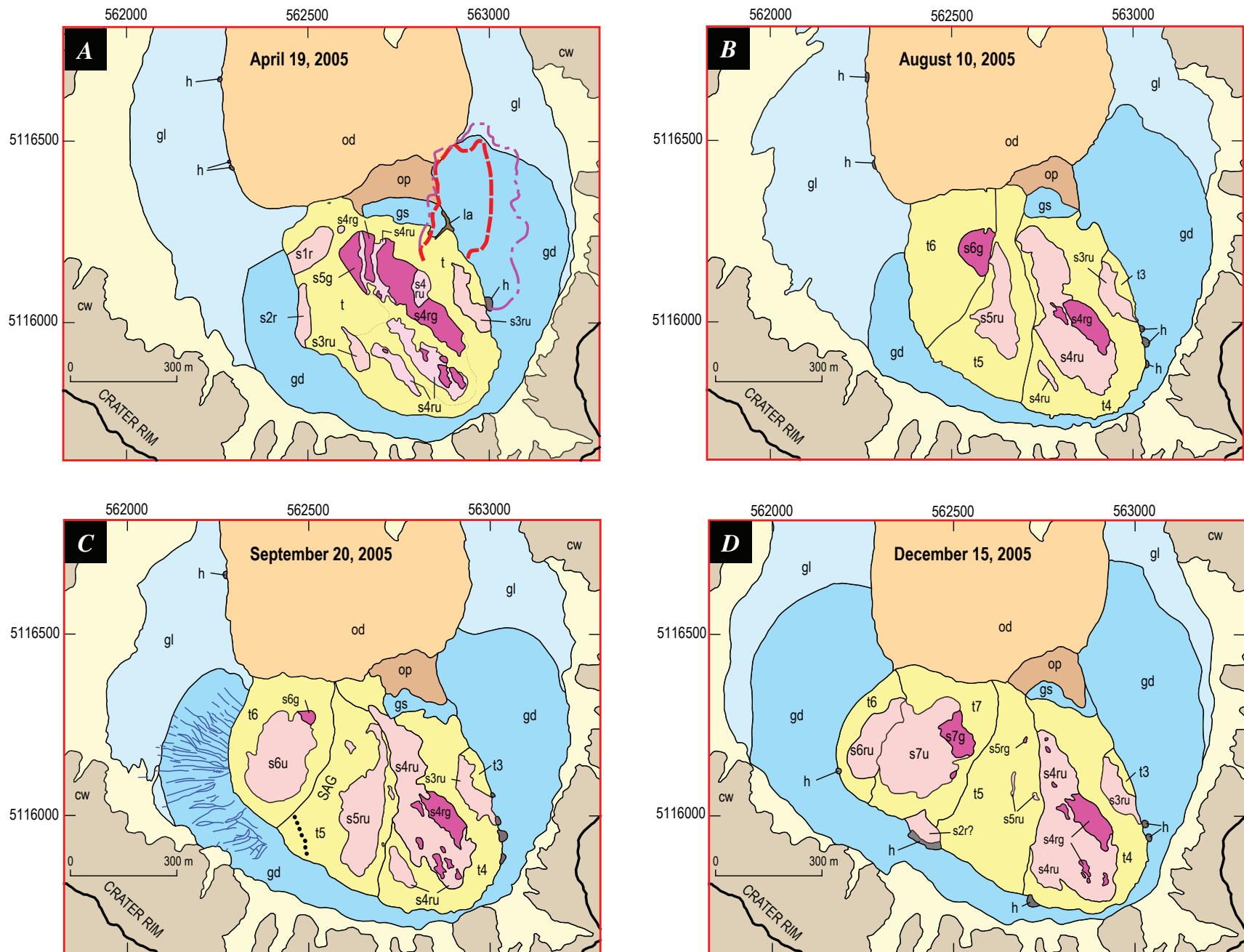
Figure 6.   Photo-based geologic map of Mount St. Helens' new dome from aerial photo taken March 10, 2005. Stars mark sample localities; see table 1.

Figure 7.   Photo-based geologic map of Mount St. Helens' new dome from aerial photo taken April 19, 2005. Stars mark sample localities; see table 1.
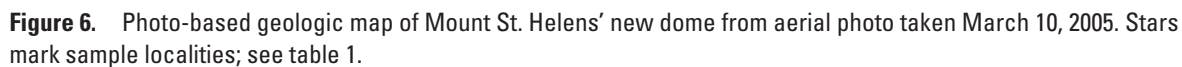
Figure 8.   Rectified geologic maps of Mount St. Helens' new dome. *A*, April 19, 2005. *B*, August 10, 2005. *C*, September 20, 2005. *D*, December 15, 2005.
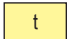
EXPLANATION
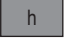
FEATURES ASSOCIATED WITH NEW DOME

s3u / s3g	Spine of 2004–2005 eruption (ongoing in December 2005)—Darker area mantled by gouge
t	Talus from flank of spine
•••••••	Steaming lineament—On figure 8*C*. Likely marks incipient renewed exposure of spine 2 from beneath mantle of talus as seen on figure 8*D*

TEPHRA DEPOSITS ON MAP OF APRIL 19, 2005

– – –	Limit, density current of ashy sediment from rockfall
– · –	Outer limit of dilute ash from rockfall

OTHER FEATURES IN CRATER

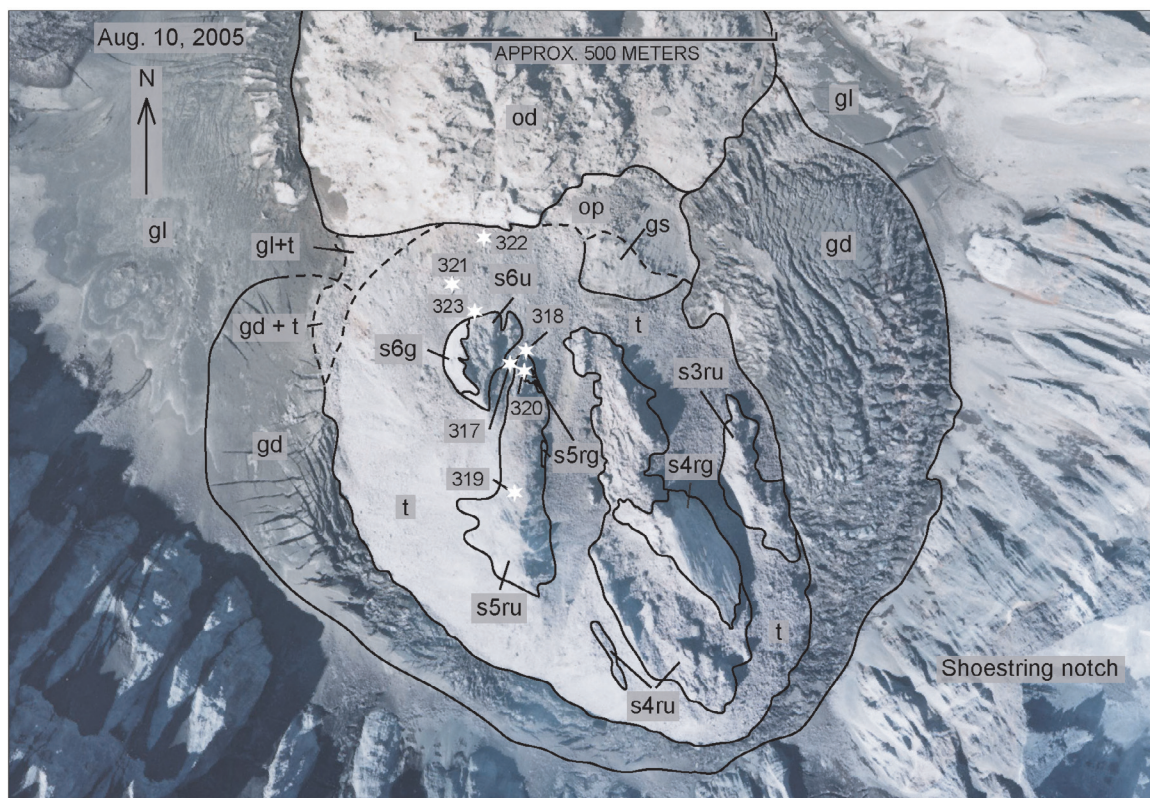|	
h	Melt pit at glacier margin
	Talus from crater walls and 1980–86 dome
gl / gd	Glacial ice—Darker area deformed by dome growth
od / op	1980–86 dome—Darker area is Opus ridge (op)
cw	Strata of crater walls and outer flanks
——	Notable crevasse on glacier—Resulting from dome emplacement. Only crevasses that developed after the previous map date are shown

Figure 8.—Continued.

Figure 9. Photo-based geologic map of Mount St. Helens' new dome from aerial photo taken August 10, 2005. Stars mark sample localities; see table 1.
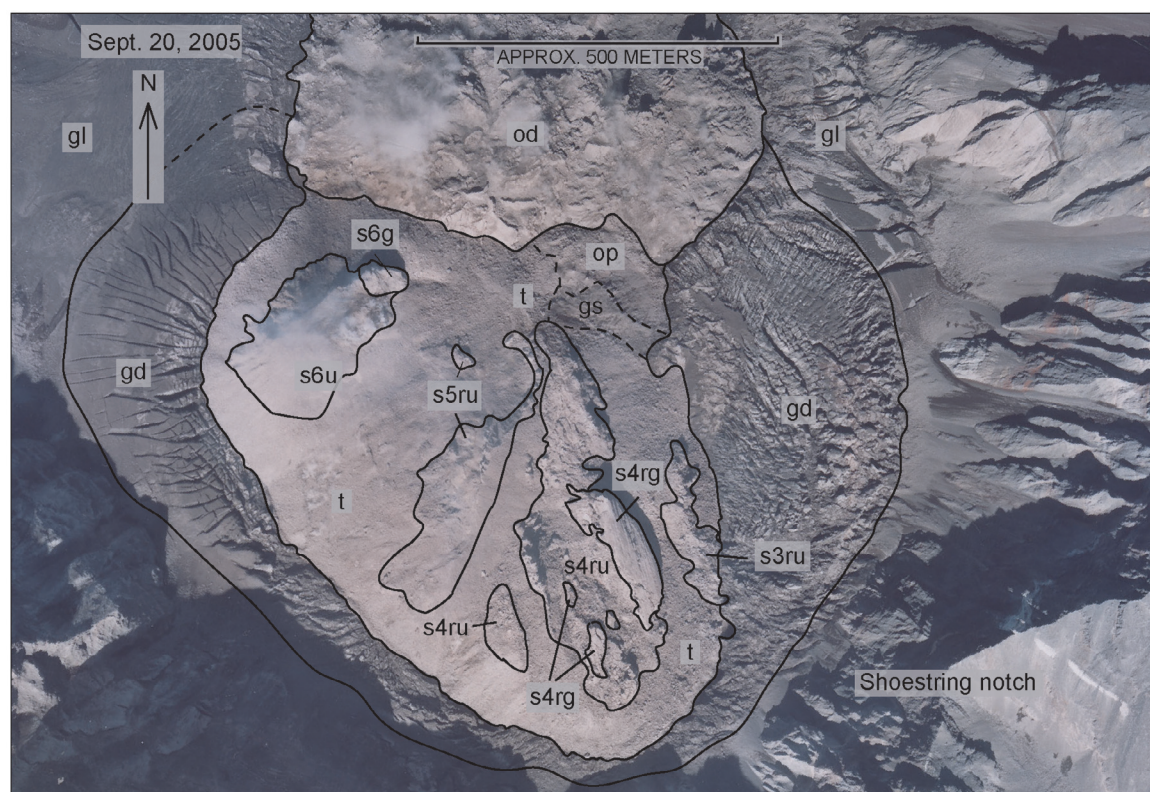

Figure 10. Photo-based geologic map of Mount St. Helens' new dome from aerial photo taken September 20, 2005.

ible only on the eastern periphery of the dome, whereas talus from spines 5 and 6 (t5, t6) now buries all remnants of spines 1, 2, and 3 to the west.

The washed-out appearance of the August 10 image (fig. 9) results from dust generated by summer rockfalls from both the new dome and the crater walls. Much of the light-dark color contrast in this photo arises from the water content of the dusted surface, which is darker where underlain by snow or ice.

September 20, 2005

Spine 6 (s6) continues to propagate westward (fig. 10). On its east side, rockfalls continue to incise the relatively small remaining parts of the gouge-mantled carapace (s6g). Abundant rockfalls from spine 5 have unroofed the core of that spine (s5ru), which now has a prominent axial crest. Spine 6's net westward motion is accompanied by subsidence between the actively growing part of the dome and the relatively stationary remnants of spines 3, 4, and 5 (fig. 8C).

Deformation in the west arm of Crater Glacier increases as spine 6 grows westward. Large new crevasses radiate outward from the contact with the expanding dome (fig. 8C). To the south, the band of glacial ice that bridges the east and west limbs of Crater Glacier has narrowed to about 6 m in width (fig. 8C).

December 15, 2005

In early October, spine 7 (s7) emerged from the sag that formed between spine 6 and remnants of spine 5 (fig. 11; Vallance and others, this volume, chap. 9). Spine 7 grew westward, pushing spine 6 remnants westward, overthrusting them, and burying them in talus. A small sliver of spine 6 (s6ru) still crops out along the margin of west Crater Glacier. Snow covers the largely cooled terrain of spines 3, 4, and 5, distinguishing it from the snow-free, hot, actively growing region of the dome. Spine 4 and 5 remnants are becoming more prominent as their cores are exhumed by rockfalls.

The deformation of Crater Glacier along its west arm is remarkable in this image (fig. 11). Deformation since August 2005 has created a jumbled serac field west of spine 6 remnants, and numerous crevasses underlie the snow-covered areas of the deformed west arm of the glacier.

Acknowledgments

Figure 11.   Photo-based geologic map of Mount St. Helens' new dome from aerial photo taken December 15, 2005.

References Cited

Dzurisin, D., Lisowski, M., Poland, M.P., Sherrod, D.R., and LaHusen, R.G., 2008, Constraints and conundrums resulting from ground-deformation measurements made during the 2004–2005 dome-building eruption of Mount St. Helens, Washington, chap. 14 *of* Sherrod, D.R., Scott, W.E., and Stauffer, P.H., eds., A volcano rekindled; the renewed eruption of Mount St. Helens, 2004–2006: U.S. Geological Survey Professional Paper 1750 (this volume).

Major, J.J., Kingsbury, C.G., Poland, M.P., and LaHusen, R.G., 2008, Extrusion rate of the Mount St. Helens lava dome estimated from terrestrial imagery, November 2004–December 2005, chap. 12 *of* Sherrod, D.R., Scott, W.E., and Stauffer, P.H., eds., A volcano rekindled; the renewed eruption of Mount St. Helens, 2004–2006: U.S. Geological Survey Professional Paper 1750 (this volume).

Pallister, J.S., Thornber, C.R., Cashman, K.V., Clynne, M.A., Lowers, H.A., Mandeville, C.W., Brownfield, I.K., and Meeker, G.P., 2008, Petrology of the 2004–2006 Mount St. Helens lava dome—implications for magmatic plumbing and eruption triggering, chap. 30 *of* Sherrod, D.R., Scott, W.E., and Stauffer, P.H., eds., A volcano rekindled; the renewed eruption of Mount St. Helens, 2004–2006: U.S. Geological Survey Professional Paper 1750 (this volume).

Poland, M.P., Dzurisin, D., LaHusen, R.G., Major, J.J., Lapcewich, D., Endo, E.T., Gooding, D.J., Schilling, S.P., and Janda, C.G., 2008, Remote camera observations of lava dome growth at Mount St. Helens, Washington, October 2004 to February 2006, chap. 11 *of* Sherrod, D.R., Scott, W.E., and Stauffer, P.H., eds., A volcano rekindled; the renewed eruption of Mount St. Helens, 2004–2006: U.S. Geological Survey Professional Paper 1750 (this volume).

Schilling, S.P., Carrara, P.E., Thompson, R.A., and Iwatsubo, E.Y., 2004, Posteruption glacier development within the crater of Mount St. Helens, Washington, USA: Quaternary Research, v. 61, no. 3, p. 325–329.

Schilling, S.P., Thompson, R.A., Messerich, J.A., and Iwatsubo, E.Y., 2008, Use of digital aerophotogrammetry to determine rates of lava dome growth, Mount St. Helens, Washington, 2004–2005, chap. 8 *of* Sherrod, D.R., Scott, W.E., and Stauffer, P.H., eds., A volcano rekindled; the renewed eruption of Mount St. Helens, 2004–2006: U.S. Geological Survey Professional Paper 1750 (this volume).

Thornber, C.R., Pallister, J.S., Rowe, M.C., McConnell, S., Herriott, T.M., Eckberg, A., Stokes, W.C., Johnson Cornelius, D., Conrey, R.M., Hannah, T., Taggart, J.E., Jr., Adams, M., Lamothe, P.J., Budahn, J.R., and Knaack, C.M., 2008, Catalog of Mount St. Helens 2004–2007 dome samples with major- and trace-element chemistry: U.S. Geological Survey Open-File Report 2008–1130, 9 p., with digital database.

Vallance, J.W., Schneider, D.J., and Schilling, S.P., 2008, Growth of the 2004–2006 lava-dome complex at Mount St. Helens, Washington, chap. 9 *of* Sherrod, D.R., Scott, W.E., and Stauffer, P.H., eds., A volcano rekindled; the renewed eruption of Mount St. Helens, 2004–2006: U.S. Geological Survey Professional Paper 1750 (this volume).

Walder, J.S., Schilling, S.P., Vallance, J.W., and LaHusen, R.G., 2008, Effects of lava-dome growth on the Crater Glacier of Mount St. Helens, Washington, chap. 13 *of* Sherrod, D.R., Scott, W.E., and Stauffer, P.H., eds., A volcano rekindled; the renewed eruption of Mount St. Helens, 2004–2006: U.S. Geological Survey Professional Paper 1750 (this volume).